International Journal of Bifurcation and Chaos, Vol. 16, No. 10 (2006) 2985–3005

PHENOMENOLOGY OF REACTION–DIFFUSION BINARY-STATE CELLULAR AUTOMATA

ANDREW ADAMATZKY
Faculty of Computing, Engineering and Mathematical Sciences, University of the West of England, Bristol, UK
andrew.adamatzky@uwe.ac.uk

GENARO JUÁREZ MARTÍNEZ
Departamento de Programación y Desarrollo de Sistemas, Escuela Superior de Cómputo, Instituto Politécnico Nacional, México DF
genarojm@correo.unam.mx

JUAN CARLOS SECK TUOH MORA
Centro de Investigación Avanzada en Ingeniería Industrial, Universidad Autónoma del Estado de Hidalgo, Pachuca, Hidalgo 42184, México
jseck@uaeh.reduaeh.mx

Received October 7, 2005; Revised October 28, 2005

We study a binary-cell-state eight-cell neighborhood two-dimensional cellular automaton model of a quasi-chemical system with a substrate and a reagent. Reactions are represented by semi-totalistic transitions rules: every cell switches from state 0 to state 1 depending on if the sum of neighbors in state 1 belongs to some specified interval, cell remains in state 1 if the sum of neighbors in state 1 belong to another specified interval. We investigate space-time dynamics of 1296 automata, establish morphology-bases classification of the rules, explore precipitating and excitatory cases and scrutinize collisions between mobile and stationary localizations (gliders, cycle life and still-life compact patterns). We explore reaction–diffusion like patterns produced as a result of collisions between localizations. Also, we propose a set of rules with complex behavior called *Life* 2*c*22.

Keywords: Cellular automata; reaction diffusion; gliders; collisions.

1. Introduction

Reaction–diffusion modeling and simulation, particularly in a sense of chemical computation and development of wave-based chemical processors [Adamatzky *et al.*, 2005a], has become a hot topic of computer science, physics and chemistry. Cellular automata are very often used as fast-prototyping tool for developing novel algorithms of wave-based computing (see e.g. [Adamatzky, 2001]). A distinctive feature of the prototyping is that it is made on an intuitive, we can say interpretative rather then implementative, level, where states are interpreted as chemical species and cell-state rules as quasi-chemical reactions [Adamatzky *et al.*, 2005b]. So we do not have to follow reaction–diffusion dynamics to simulate it in automata [Toffoli & Margolus, 1987] but instead we should map all possible models of cellular automata onto a space of quasi-chemical reactions. The quest will bring not only original designs of reaction–diffusion computers but also an answer to the long-standing (from von Neumann's model of chemical automata [von Neumann, 1966])

questions of how reaction–diffusion relates to self-reproduction and universal computation, and a role of primitive structures in shaping spatio-temporal mosaic of emergent complex behavior [Langton, 1984; Wuensche, 2004]), better known as gliders, mobile self-localizations or particles.

A well known variety of evolution rules support behavior similar to reaction and diffusion, see [Packard & Wolfram, 1985] and [Maginer *et al.*, 1997], however, so far no one has undertaken a systematic analysis of "reaction–diffusion" rules, particularly in terms of constructing parametric space, establishing conditions of pattern formation, and studying how patterns may be formed in collision with mobile self-localizations or gliders.[1]

In this paper, we consider the simplest possible model of a quasi-chemical system — two-dimensional cellular automaton, where every cell has eight neighbors and updates its states depending on whether the sum of neighbors in state 1 belongs to certain intervals. In Sec. 2 we study automaton, where state 1 is an absorbing state, so when in state 1 cell never leave the state; this is a model of simple precipitation. Morphological classification[2] of semi-totalistic cell-state transition rules is provided in Sec. 3, where we study a model of diffusion and reaction in quasi-chemical system. Section 4 specifies rules that support self-localizations (compact patterns traveling undisturbed, like solitons in optical media [Adamatzky, 2001; Jakubowski *et al.*, 2001] or gliders in Conway's Game of Life [Gardner, 1970]). Reaction–diffusion patterns generated as a result of collisions between localizations (gliders and cycle life) are analyzed in Sec. 5, where we propose a set of rules able to support complex behavior, called "Life 2*c*22." Yet another class of automata, based on a particular behavior of cells in state 1 is studied in Sec. 6, there a cell in state 1 takes state 0 independent of states of its neighbors. More ideas on reaction–diffusion automata and plans for future studies are tackled in Sec. 7.

2. Patterns of Precipitation

We study a two-dimensional (2D) cellular automaton (CA), where every central cell $x \in \mathbb{Z} \times \mathbb{Z}$ (where $\mathbb{Z}$ is an integer set), has eight neighbors (Moore neighborhood), so that $u(x) = \{y \in \mathbb{Z} : x \neq y$ and $|x - y| \leq 1\}$, and takes two states, 0 and 1. Let σ_x^t be a sum of cells in state 1 in neighborhood $u(x)$ of cell x at time step t. Every cell updates its state by the rule:

$$x^{t+1} = \begin{cases} 1, & \text{if } (x^t = 0 \text{ and } \sigma_x^t \in [\theta_1, \theta_2]) \text{ or } (x^t = 1) \\ 0, & \text{otherwise} \end{cases} \tag{1}$$

A cell in state 0 takes state 1 if the number of its neighbors in state 1 belong to interval $[\theta_1, \theta_2]$, $1 \leq \theta_1 \leq \theta_2 \leq 8$; once in state 1 a cell remains in this state forever. The model represents a quasi-chemical precipitating system, where 0 is a substrate and 1 is a reagent, when reagent diffuses onto the substrate it is bound to substrate, a kind of precipitation occurs. We can call interval $[\theta_1, \theta_2]$ a precipitation interval. Examples of configurations generated by CA cell transitions of which are governed by various values of θ_1 and θ_2 are shown in Fig. 1.

For narrow precipitation intervals with small lower boundaries, $[1, 1]$, $[1, 2]$, $[2, 2]$, structures formed by precipitate, cells in state 1, resemble intersection and overlapping branching tress (see configurations marked $[1, 1]$, $[1, 2]$ and $[2, 2]$ in Fig. 1). The complex structure of branching structures is produced because every cell in state 1 or two neighboring cells in state one (in the initial configuration) generate a multiply-branching trees of precipitate, see Figs. 2(a)–2(c).

Further increase of upper boundary, $[1, 3]$ and $[1, 4]$, and lower boundary, $[2, 3]$, $[2, 4]$, $[3, 3]$ and $[3, 4]$ leads to formation of Voronoi-like domains around each cell that was in state 1 initially (see more details about CA generation of Voronoi diagrams in [Adamatzky, 2001]). Edges of Voronoi diagrams (see white domains in configurations signed by $[1, 3], [1, 4], [2, 3], [2, 4], [3, 3], [3, 4]$ in Fig. 1, and particularly configuration $[3, 4]$) are represented by narrow domains of cells in state 0). This happens because at sites where fronts of precipitation (originating from different sources) approach each other, cells in state 0, "squeezed" between the fronts, have number of 1-state neighbors exceeding θ_2 and so these cells do not take state 1 (Fig. 3).

When lower boundary of "precipitation" interval $[\theta_1, \theta_2]$ becomes more than 3, typical configuration of CA developing from random initial configuration is a population of mostly sparsely

[1]We used terminology of the automaton discovered by John Horton Conway — The Game of Life [Gardner, 1970].
[2]The full catalogue of nontrivial patterns is available at http://uncomp.uwe.ac.uk/adamatzky/q2d1d2t1t2/appendix.pdf

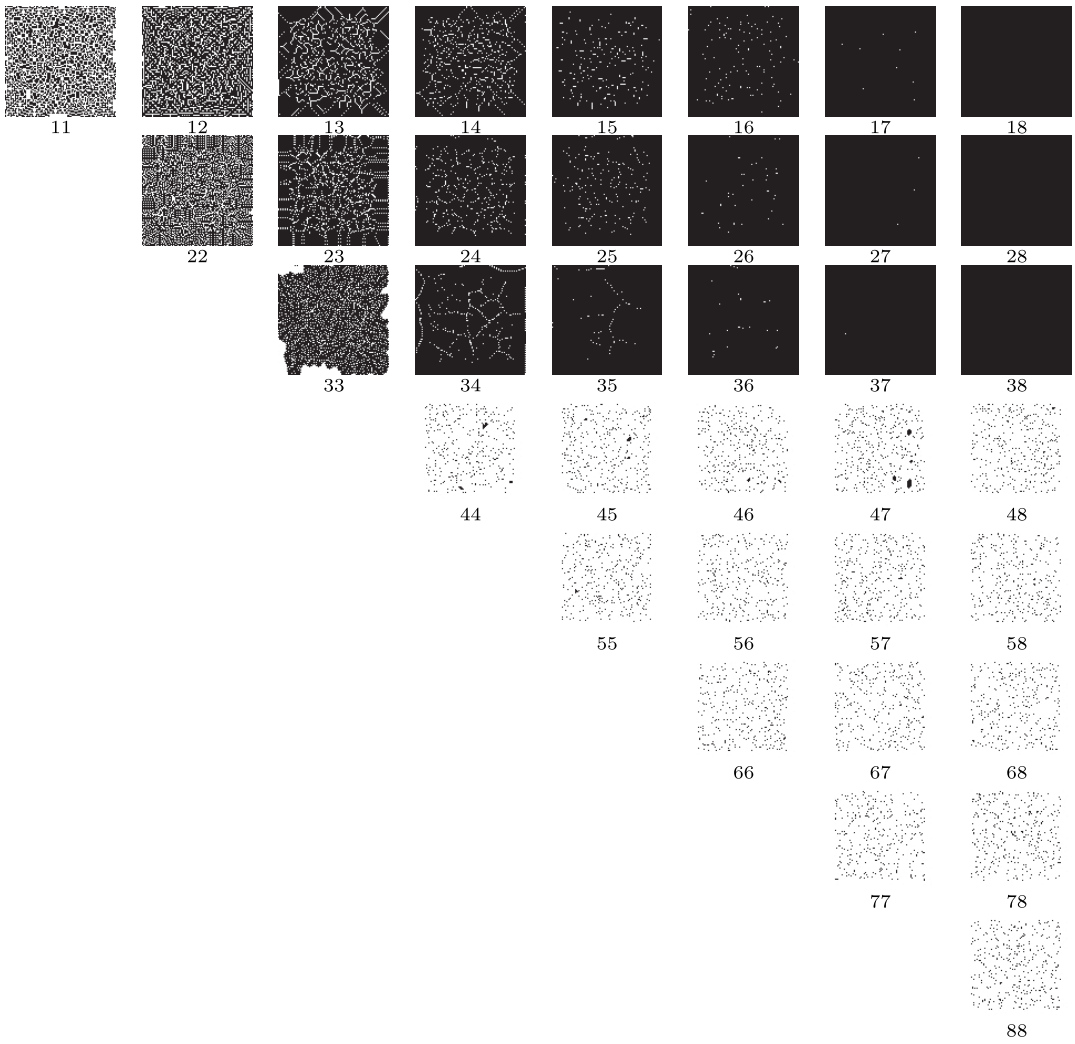

Fig. 1. Configurations of 2D 100×100 cells "precipitating" CA, developed from initial random configuration (with 10% of cells in state 1) after 100 steps; each configuration is signed with two digits representing values of θ_1 and θ_2.

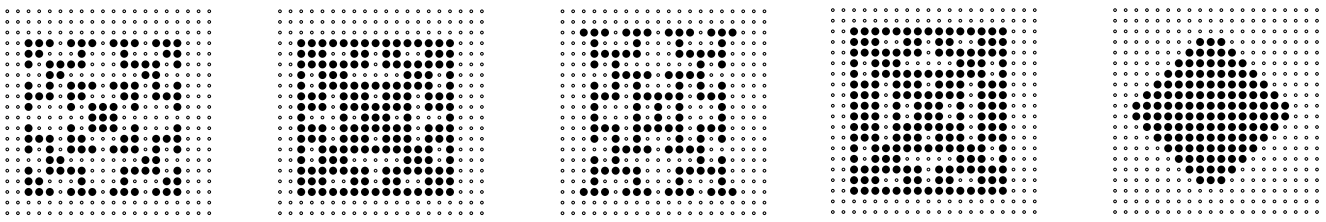

Fig. 2. Configuration of 2D $n \times n = 20 \times 20$ cells "precipitating" CA developed from initial configuration where all sites are in state 0 but the only center cell is in state 1. Configuration displayed at time step $t = 7$. Cells in state 1 are shown in discs, in state 0 by dots. Initially, $t = 0$, all cells but those indicated below are in state 0. (a) $\theta_1 = \theta_2 = 1$, $x^0_{n/2,n/2} = 1$, (b) $\theta_1 = 1, \theta_2 = 2$, $x^0_{n/2,n/2} = 1$, (c) $\theta_1 = \theta_2 = 1$, $x^0_{n/2,n/2} = 1$ and $x^0_{n/2,n/2+1} = 1$, (d) $\theta_1 = 1, \theta_2 = 2$, $x^0_{n/2,n/2} = 1$ and $x^0_{n/2,n/2+1} = 1$, (e) $\theta_1 = 2, \theta_2 = 3$, $x^0_{n/2,n/2} = 1$ and $x^0_{n/2,n/2+1} = 1$.

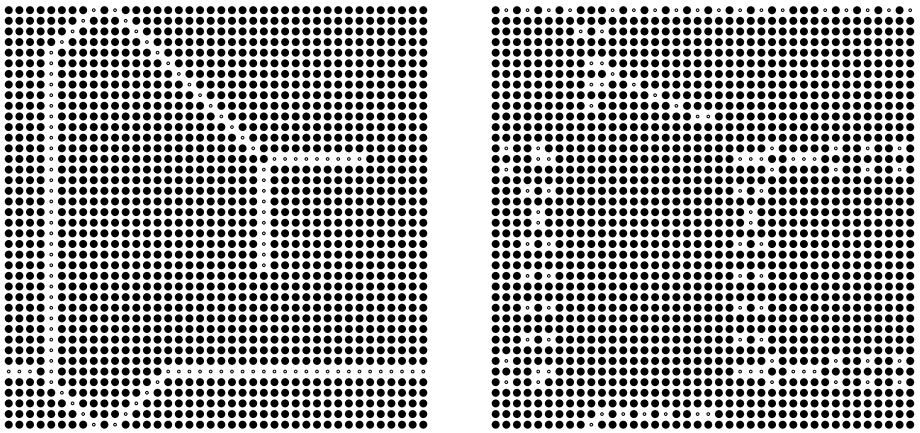

(a) (b)

Fig. 3. Configuration of $n \times n = 40 \times 40$ CA recorded at step $t = 40$, the automata started their development in configuration where almost all cells were in state 0 but cells with coordinates $(n/2, n/2)$, $(n/2, n/2+1)$, $(n/2+n/4, n/2)$, $(n/2+n/4, n/2+1)$, $(n/2+n/4, n/2+1+n/4)$ and $(n/2+n/4, n/2+1+n/4+1)$ were in state 1. (a) $\theta_1 = 1$ and $\theta_2 = 3$, (b) $\theta_1 = 2$ and $\theta_2 = 3$.

distributed states 1 (black pixels in Fig. 1). This is because in sparse random initial configuration a cell in state 1 is usually surrounded by neighbors in state 0 and therefore initial random configuration remains in general unchanged during automaton development.

For every value of intervals' boundaries and any initial condition the automaton eventually gets trapped in a fixed point of evolution, where no cell changes its state (because 1 is an "absorbing" cell state, or a precipitate). To make things more attractive dynamically we can allow for "dissociation" of reagent "1" from substrate "0", the model is discussed in the following section.

3. Phenomenology of Diffusion and Reaction

Let σ_x^t be a sum of cells in state 1 in neighborhood $u(x)$ of cell x at time step t, and $0 \leq \theta_1 \leq \theta_2 \leq 8$ and $0 \leq \delta_1 \leq \delta_2 \leq 8$. Every cell x updates its state x^t by the following rule:

$$x^{t+1} = \begin{cases} 1, & \text{if } (x^t = 0 \text{ and } \sigma_x^t \in [\theta_1, \theta_2]) \text{ or} \\ & \quad (x^t = 1 \text{ and } \sigma_x^t \in [\delta_1, \delta_2]) \\ 0, & \text{otherwise} \end{cases} \qquad (2)$$

Selecting particular values of intervals' boundaries we change cell state transition rule, and subsequently the development of space-time dynamics in the automaton. In this paper, we specify the form $R(\delta_1, \delta_2, \theta_1, \theta_2)$. The rule can be interpreted as a simple discrete model of a quasi-chemical system with substrate "0" and reagent "1", and $[\theta_1, \theta_2]$ is analogous to diffusion rate, or in association between substrate and reagent, and $[\delta_1, \delta_2]$ is analogous to a reaction rate, or as in other terms with a degree of affinity between substrate and reagent.[3]

We analyzed patterns produced by each of 1296 rules, from initially random configuration (the same random configurations were used for all rules) where every cell was assigned state 1 with probability 0.3, cell state transitions Eq. (2) for all possible values of intervals' boundaries. Several morphology-based classes of rules are discovered.[4]

The rules which transform random initial configuration to a uniform configuration of cells in state 0 are grouped in the **E**-class. For example, rules $R(33ab)$, $a \geq 5$, $b \geq 5$ (it is assumed that $a \leq b$, $a, b \leq 8$); $R(44ab)$, $a, b \geq 4$; $R(4cab)$, $a, b \geq 4$, $c = 4, 5$. The interval boundaries of the rules are so that initial 1-states do not spread to neighboring 0-state sites, and cells in state 1 could not be in this state for longer than a few time steps of development. The class **E** represents a quasi-chemical system with sub-threshold diffusion and reaction rates.

[3]The model is a generalization of Conway's Game of Life, where $[\theta_1, \theta_2]$ and $[\delta_1, \delta_2]$ are intervals of birth and survival; the Game of Life rule can be written as $R(2333)$ or $S23/B33$.

[4]You can reproduce each CA with our OSX2DCASM system available from http://uncomp.uwe.ac.uk/genaro/OSXCASystems.html

The second class — **S**-class — is comprised of rules which almost did not change initially the random configurations. Small clusters of 1-states are formed but never spread for more than a few cells, e.g. configurations generated by rules $R(11ab)$, $a, b \geq 3$ or $R(22ab)$, $a, b \geq 4$. Diffusion rate is still low for substantial patterns to form but reaction rate is high enough to keep formed patterns stable.

The third simple class, **D**, comprised of rules that generate solid (all almost solid) configurations, where the whole lattice is filled with 1-states. For example, the class includes rules $R(d8a8)$, $1 \leq a \leq 4$, $d = 2, 3$ and $R(d8a8)$, $1 \leq a \leq 3$, $d = 4, 5$; the rule represent high reaction and diffusion rates.

L-class includes rules that generate fine labyrinths of 1-states. Some exemplar configurations are shown in Fig. 4. There are at least two distinctive types of structures: $\mathcal{L}_1$-labyrinths with walls one cell sick [see e.g. Figs. 4(a) and 4(b)], and $\mathcal{L}_2$-labyrinths with walls few cells sick [see e.g. Figs. 4(c) and 4(d)]. $\mathcal{L}_1$ labyrinths are formed because diffusion rate, interval $[\theta_1, \theta_2]$ is narrow enough to allow only stripes of 1-states to grow and join each other, and the one cell wide stripes are stabilized by reaction rate, interval $[\delta_1, \delta_2]$ allowing for only cells surrounded by, e.g. one, two or three neighbors in 1-state to persist. Decreasing reaction interval, e.g. going from rule $R(1312)$ to rule $R(1322)$, dramatically reduces the amount of free hanging ends of stripes (where cell in state 1 has just one neighbor, as in Fig. 4(a)) and therefore development favors continuous (but possibly frequently turning) stripes [see Fig. 4(b)]. Increasing upper boundary of reaction interval $[\delta_1, \delta_2]$ leads to formation of sick stripes, $\mathcal{L}_2$-labyrinths, see e.g. Figs. 4(c) and 4(d). Formation of $\mathcal{L}_2$-labyrinths may be attributed to high degree of diffusion and relatively high rate reactions compared to that in medium's producing $\mathcal{L}_1$-labyrinths.

With increase of both lower and upper boundaries of diffusion interval $[\theta_1, \theta_2]$ we see formation of irregularly oriented and often branching stripe-like domains of 1-states, examples are shown in Fig. 5. We group the rules generating such patterns

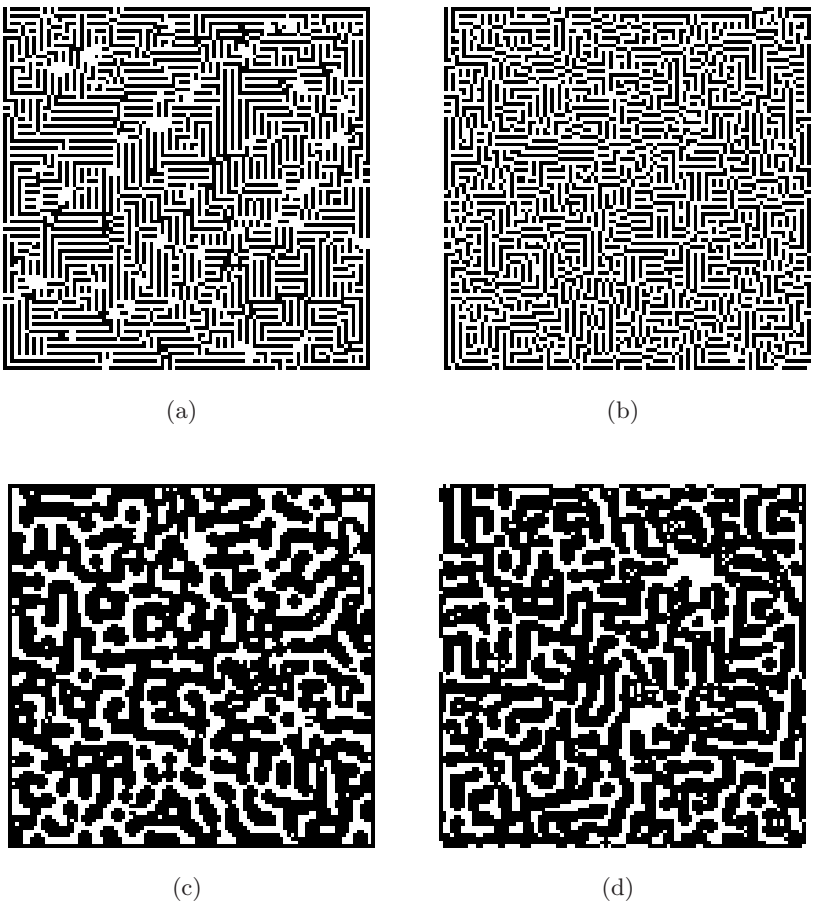

Fig. 4. Examples of configurations generated by rules of **L**-class. (a) $R(1312)$, (b) $R(1322)$, (c) $R(1616)$, (d) $R(4617)$.

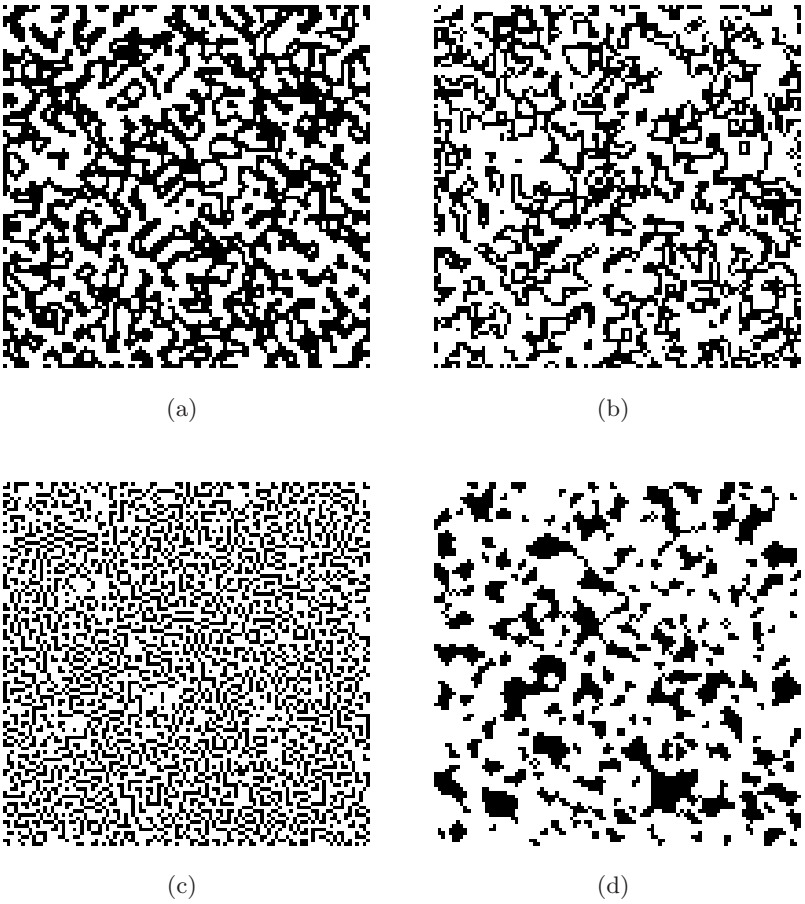

Fig. 5. Examples of configurations generated by rules of **M**-class. (a) $R(1315)$, (b) $R(1425)$, (c) $R(2213)$, (d) $R(2858)$.

to **M**-class. The strips become thinner with decrease of diffusion rate, see transitions between configurations (a) → (b) → (c) in Fig. 5, and they are transformed to interconnected domains with increase of diffusion rate and increase of lower boundary of reaction interval [Fig. 5(d)].

Rules representing high diffusion rate (wide interval $[\theta_1, \theta_2]$) and low reaction rate (narrow $[\delta_1, \delta_2]$) generate configurations where domains of mostly 0-states with scattered 1-states compete with domains of mostly 1-states with scattered 0-states (Fig. 6). The rules are grouped in **P**-class.

Configurations of irregularly distributed spots (domains of fews cells in 1-state) are typically generated by rule in **O**-class. The spots may be connected by thin filaments of 1-states. The rules represent very low rate of diffusion (self-inhibiting diffusion) and high reaction rate (Fig. 7).

Three more classes can be specified but now based on computational functionality of developing configurations. Here, we follow a paradigm of reaction–diffusion computing, where data are represented by initial concentrations of reagents, computation is implemented by spreading and interacting patters (e.g. diffusion or excitation waves), and the result is given by final (either stationary or oscillating) distribution of reagents (see details in [Adamatzky, 2001]). In automaton classes studied in this paper, computationally functional rules are morphologically indistinguishable from "computationally useless" rules.

The first, computationally functional class **G** consists of rules $R(2c22)$, where $2 \leq c \leq 8$. The rules support mobile localizations, or gliders, in CA development. By colliding gliders we can implement any kind of logical operations, as well studied in the field of collision-based computing, see [Adamatzky, 2003]. Particulars of interaction between localizations will be discussed in detail in Sec. 4. Other examples of functionally complete — collision-based — binary-state automata include Conway's Game of Life [Berlekamp *et al.*, 1982], HighLife (modification of Game of Life where $0 \rightarrow 1$ transition happens if there are either three or six

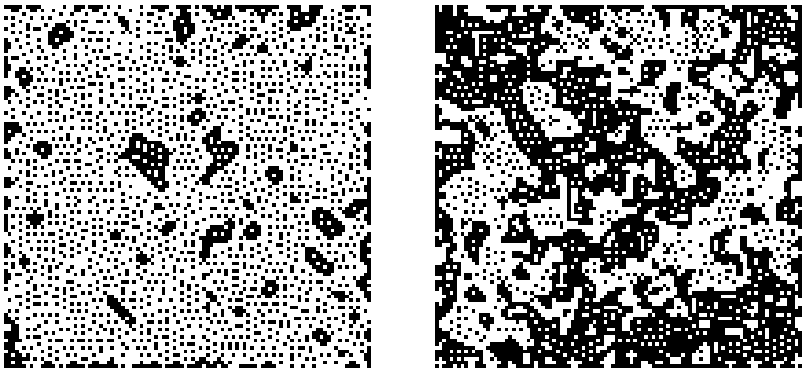

(a) (b)

Fig. 6. Examples of configurations generated by rules of **P**-class. (a) $R(2318)$, (b) $R(2418)$.

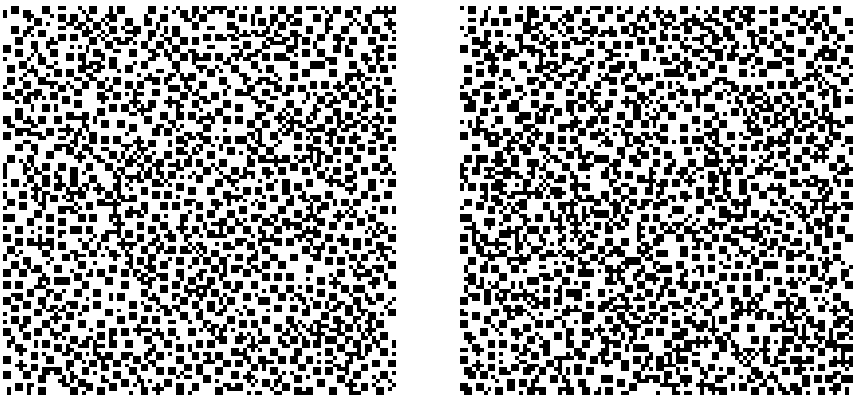

(a) (b)

Fig. 7. Examples of configurations generated by rules of **O**-class. (a) $R(3511)$, (b) $R(3811)$.

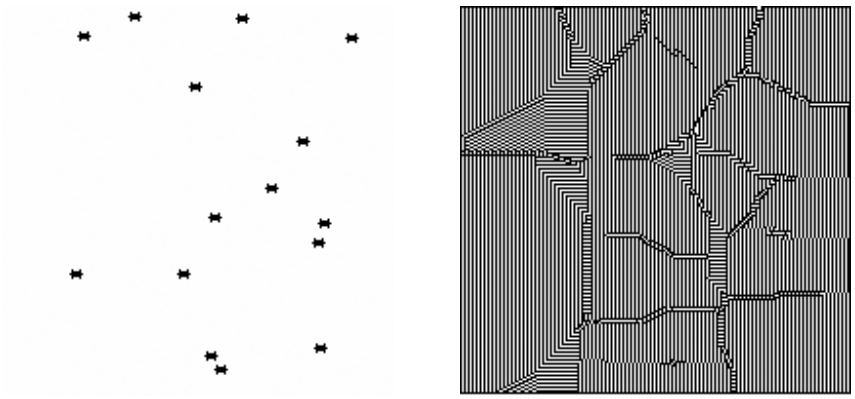

(a) (b)

Fig. 8. Partial construction of Voronoi diagram in CA governed by rules (b) $R(1634)$, (c) $R(1834)$, (d) $R(4834)$, initial data set represented by domains of six cells in 1-state is shown in (a).

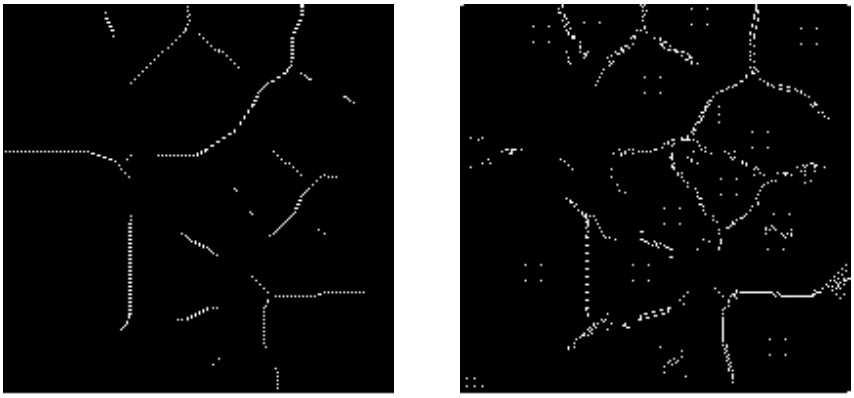

(c) (d)

Fig. 8. (*Continued*)

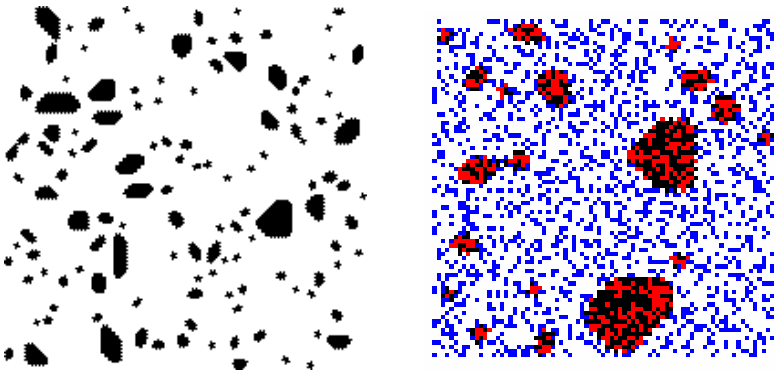

(a) (b)

Fig. 9. Constructing convex hull by CA rule $R(4848)$, (a) a typical final configuration for initial random configuration where every cell took state 1 with probability 0.3; (b) superposition of initial random configuration, gray pixels are cells in state 1, and black domains are final configurations.

neighbors in state 1, and transition $1 \rightarrow 1$ if there are two or three neighbors in state 1) [Bell, 1994].

A set of rules grouped in class **V** allows for partial computation or approximation of a Voronoi diagram — given a set of planar points compute such domain for each point p of data set that any point in the domain is closer to p than to any other point of a given data set. Boundaries of the domains constitute Voronoi diagram. See details of constructing Voronoi diagram in chemical reaction–diffusion systems in [Adamatzky, 2001]. As you can see in Fig. 8 edges of Voronoi diagram can be represented either by loci without reagent, i.e. domains of cells in state 0 [Figs. 8(c) and 8(d)], or by different types of tiling [Fig. 8(b)].

Rules grouped in class **C** approximate discrete convex hulls (see [Adamatzky, 1995] for formal background) of connected subsets of cells being initially in 1-state, so an initially random configuration of 1-state cells is transformed by the rules of **G** to a set of discrete convex hulls of various sizes (Fig. 9). The class includes rules $R(4847)$ and $R(4848)$.

4. Rules Supporting Gliders: *Life* 2*c*22

Analyzing space-time dynamics of the automata we found a subset of rules that support a wide range of stationary and mobile localizations like: gliders, cycle life, still life and puffer trains.[5] The subset

[5]We use notations typical for Game of Life literature, see e.g. http://pentadecathlon.com/index.shtml.

of evolution rules called Life 2c22 is represented as $R(2c22)$, where c takes values of 2 to 8, i.e. $R(2222), \ldots, R(2822)$. They have very narrow intervals of diffusion $[\theta_1, \theta_2] = [2, 2]$ and a wide range of reaction parameters, $2 \leq \delta_1 \leq \delta_2 \leq 8$. We have found that there is no difference in localizations generated by rules $R(2722)$ and $R(2822)$, so for these two rules we consider only $c = 7$.

The basic mobile localization is a glider period one (Fig. 10) existing for all rules of Life 2c22. All gliders and puffer trains in Life 2c22 travel in four directions: south, north, east and west.

The basic stationary localizations include blinkers of period two and four, see Fig. 11. Smallest

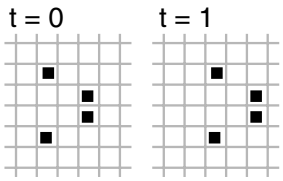

Fig. 10. Glider of period one.

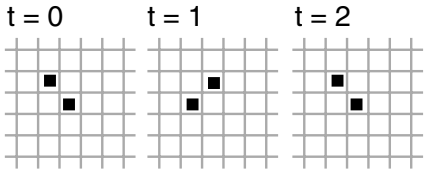

(a)

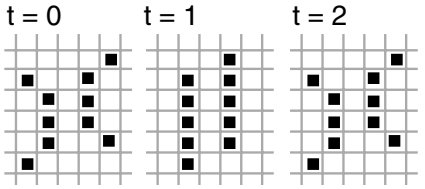

(b)

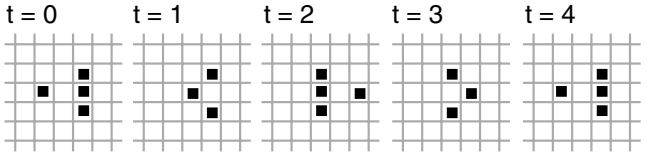

(c)

Fig. 11. Stationary localizations (cycle life) of: (a) and (b) of period two, (c) period four.

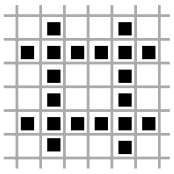

Fig. 12. Still life configuration.

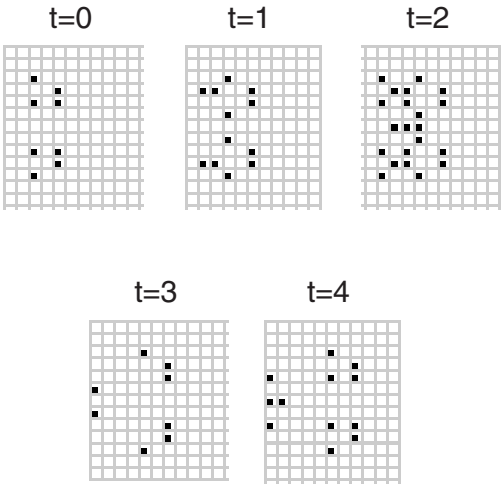

Fig. 13. Puffer train configuration.

still localization is a "still life" occupying 20 cells (see Fig. 12), and a puffer train of period four (see Fig. 13),[6] both structures exist for Life 2c22 where $4 \leq c \leq 8$.

Figures 14 and 15 show the behavior of Life 2c22, each automaton starts its development from a random initial condition with low density (approximately 0.01). In the opposite case, we found that to observe interesting behavior of gliders it is better to keep the initial density of 1-states between 0.85, for $2 \leq c \leq 3$, and 0.93, for $4 \leq c \leq 5$.

In Life 2c22 we can observe the generation of few gliders and blinkers, mainly when c is smaller and several catastrophes are initiated. Notably the catastrophes induced by collision of gliders destroy the fragile "ecosystem" of co-existing localizations. This is the reason why some of the localizations studied were never discovered before, because they only exist during short periods of initial evolution and extreme densities. Thus even in our morphological classification, see Sec. 3, the glider-supporting rules were grouped to **M-class**, renowned for "unstructured", chaotic-like, configurations.

[6]Puffer train was discovered by Adriana Menchaca and Miriam Mecate.

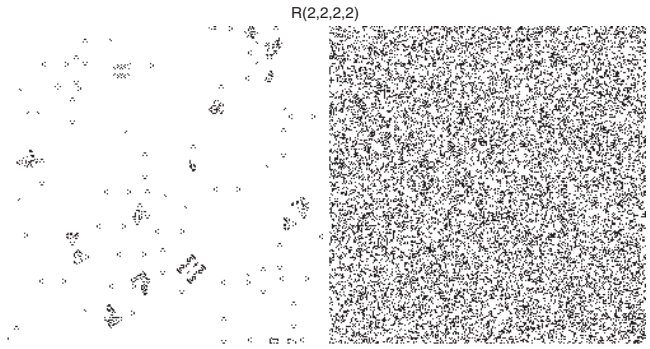

(a)

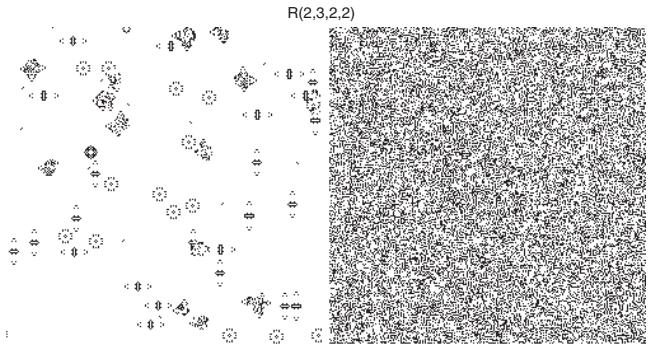

(b)

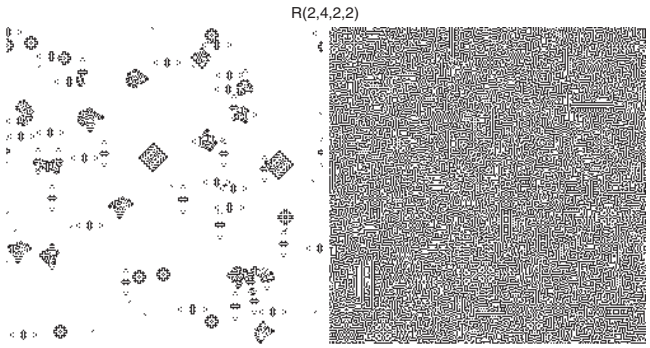

(c)

Fig. 14. Random initial condition with low density, first configuration for each Life $2c22$, $c = 2, 3, 4$, shows the development of CA, 300×300 cells, after 10 steps, gliders and blinkers are easily detectable, the second configuration shows the final state of the automaton.

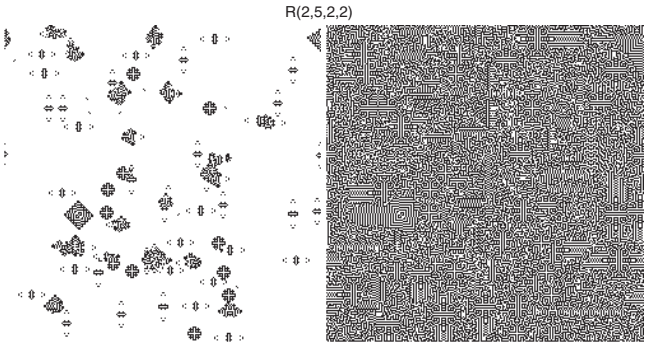

(a)

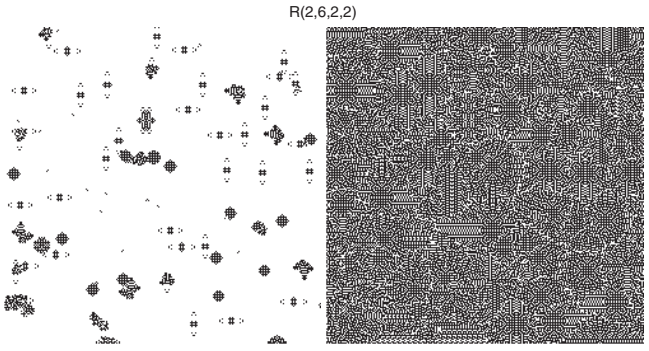

(b)

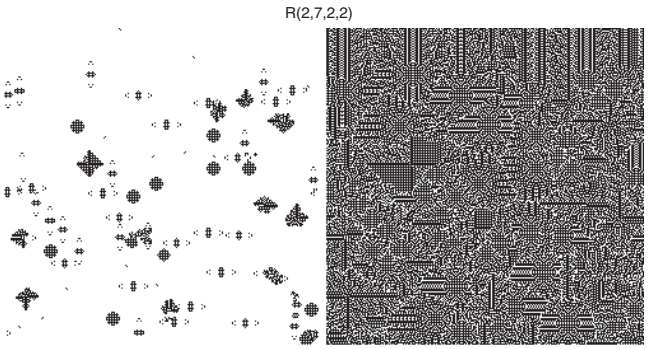

(c)

Fig. 15. Random initial condition with low density, first configuration for each Life $2c22$, $c = 5, 6, 7$, shows the development of CA, 300×300 cells, after 10 steps, gliders and blinkers are easily detectable, second configuration shows the final state of the automaton.

5. Collision-Induced Pattern Formation

It is well known that for certain initial conditions some cell-state transition rules produce patterns bearing striking resemblance to "living" reaction–diffusion systems (even in this particular study we observed Turing-like structures [Turing, 1952; Yang *et al.*, 2004]), however so far there has been no published results about the generation of growing reaction–diffusion patterns by collisions between gliders. This is discussed in the present section.

Before proceeding to findings of the systematic analysis we would like to highlight basic interactions between gliders.

In Life 2c22 we found that when two gliders collide — we mean head-on collision, even distance, side shift one — they annihilate; this collision happens for all rules of $R(2c22)$, see Fig. 16. In other cases, they produce a blinker see Fig. 17.[7]

If we grouped four gliders, each one in four directions, then we have multiple collisions, the results of which depend on values of c as demonstrated in Fig. 18. Another exercise adopted from Game of Life studies is to arrange the line of 1-states and analyze structures produced, in such a way we can, e.g. see in rule $R(2433)$ a circular growth initiated by seven cells in state 1 [Wolfram, 2002].

In Fig. 19, we see that the initial configuration of two cells in state 1 generates two gliders, traveling in opposite directions, and also, for $c > 2$ a reaction–diffusion like pattern spreading all over the lattice.

Exemplar outcomes of head-on odd-distance nil-offset collision of gliders are shown in Fig. 20, all reaction–diffusion patterns generated are highly symmetric however the symmetry is hidden behind quasi-irregularity of the patterns for $c = 2, 3$.

Increasing the number of colliding gliders, see in Fig. 21, makes no significant change in morphology of patterns generated but affects symmetries of the patterns. The collision in Fig. 21 is particularly interesting, because it makes an impression that the glider initially traveling north continues its

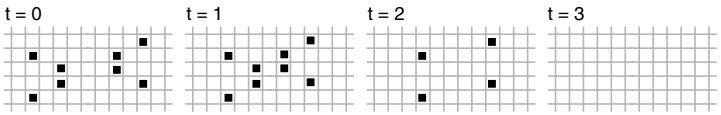

Fig. 16. Annihilation of gliders in collision with Life 2c22.

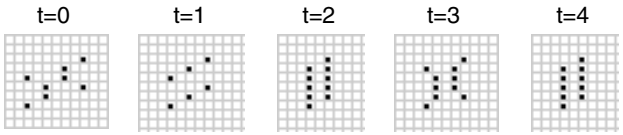

Fig. 17. Producing a blinker to Life 2c22.

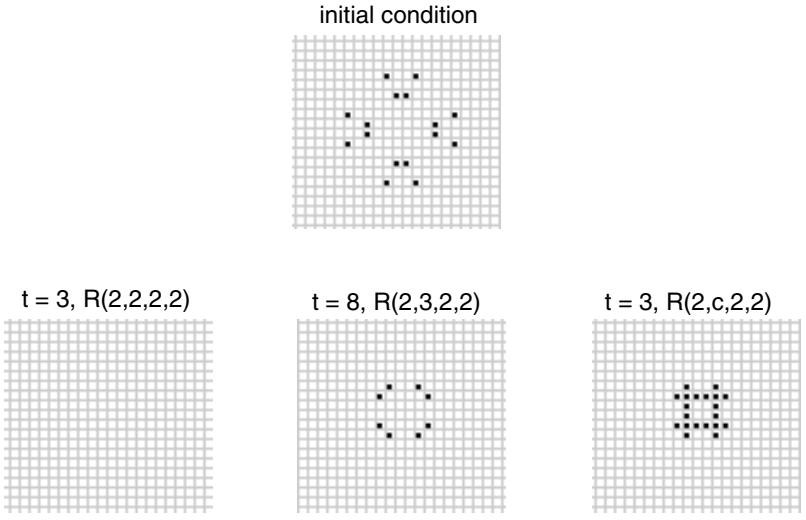

Fig. 18. Four gliders annihilate ($c = 2$), produce four blinkers ($c = 4$) and one still life ($4 \leq c \leq 8$).

[7]Collision producing blinker was discovered by Miriam Mecate and Adriana Menchaca. All binary collisions between gliders are available from http://uncomp.uwe.ac.uk/genaro/diffusionLife/life_2c22.html

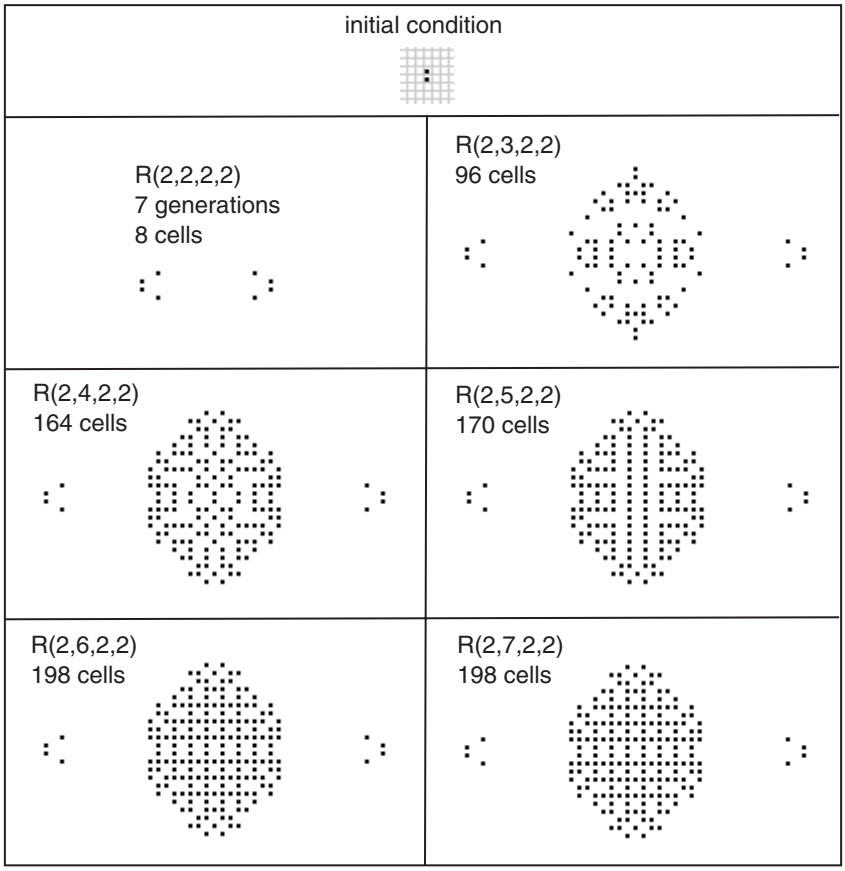

Fig. 19. Initial configuration with two cells in state 1 produces two gliders, however for $c > 2$ a reaction–diffusion pattern is also initiated but spreads more slowly than traveling gliders.

journey undisturbed (may be with some delay) but gliders traveling east and west are both diverted south.

Outcomes of glider collision with two blinkers are shown in Fig. 22. For rule $R(2222)$ the glider is multiplied, and the three gliders continue traveling east, at the same time a disordered rhomboid pattern starts to grow. For $c = 3$ two gliders traveling north and south are formed, but the growing reaction–diffusion pattern still remains

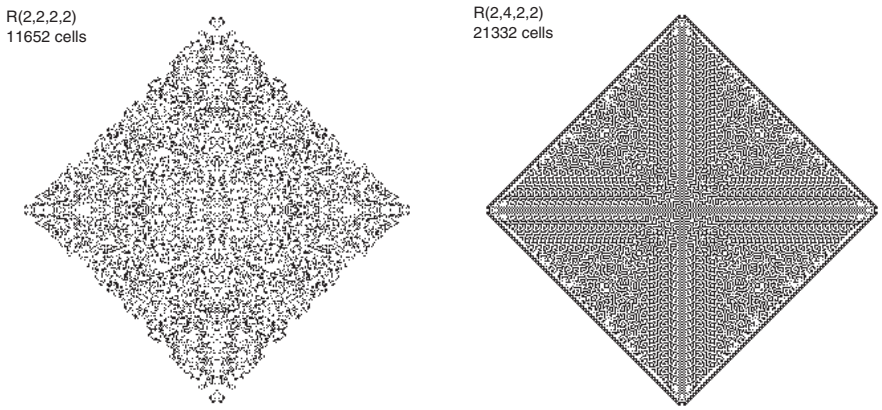

(a) (b)

Fig. 20. Examples of patterns produced in collision of two gliders, head-on collision, odd distance between gliders, nil side shifts. The configurations are recorded at 150th step to each Life 2c22.

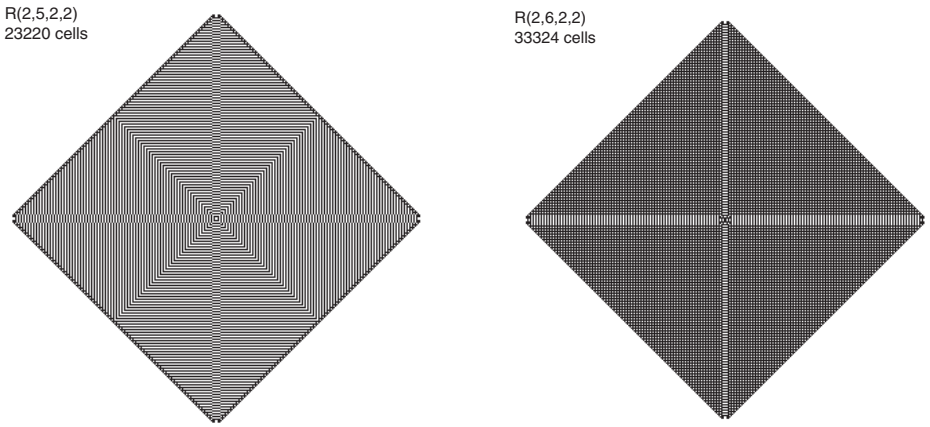

(c) (d)

Fig. 20. (*Continued*).

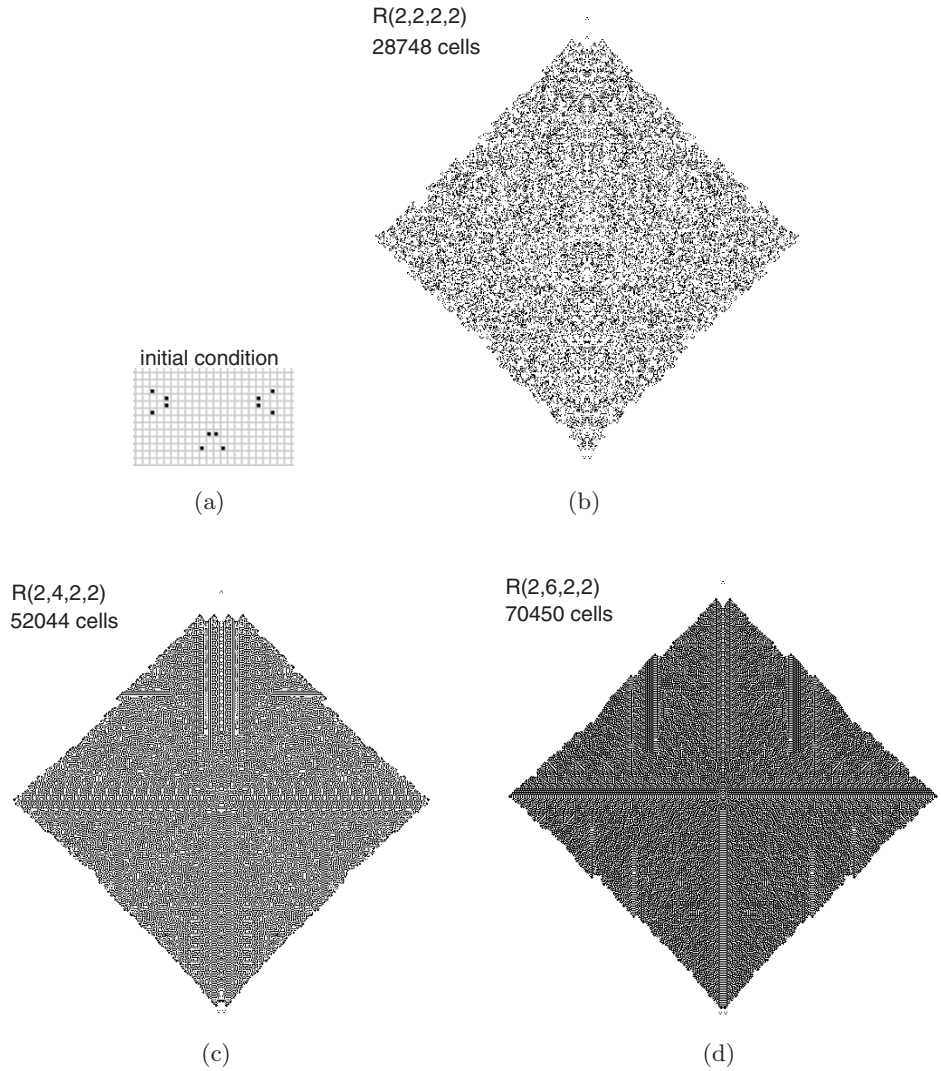

(a) (b)

(c) (d)

Fig. 21. Exemplar patterns generated in collision between three gliders, initial disposition of gliders is shown in (a), gliders traveling south and north are also produced, they are followed by the growing reaction–diffusion pattern.

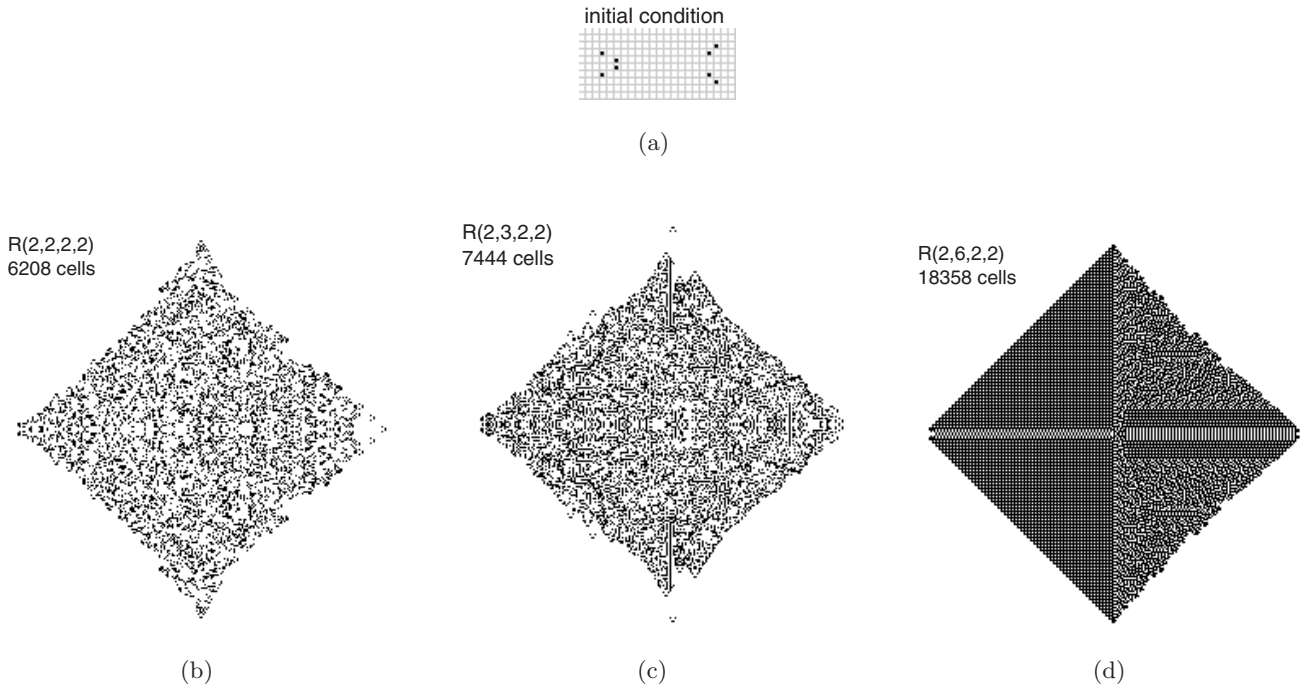

Fig. 22. Examples of collision of glider traveling east to two blinkers (a). Configurations that emerged as a result of the collision are recorded at 125th step of CA development. The initial trajectory of the glider determines a periodic domain on the western part of each configuration whereas positions of blinkers are somewhat responsible for a mixture between chaotic and periodic domains in the eastern part of the growing pattern.

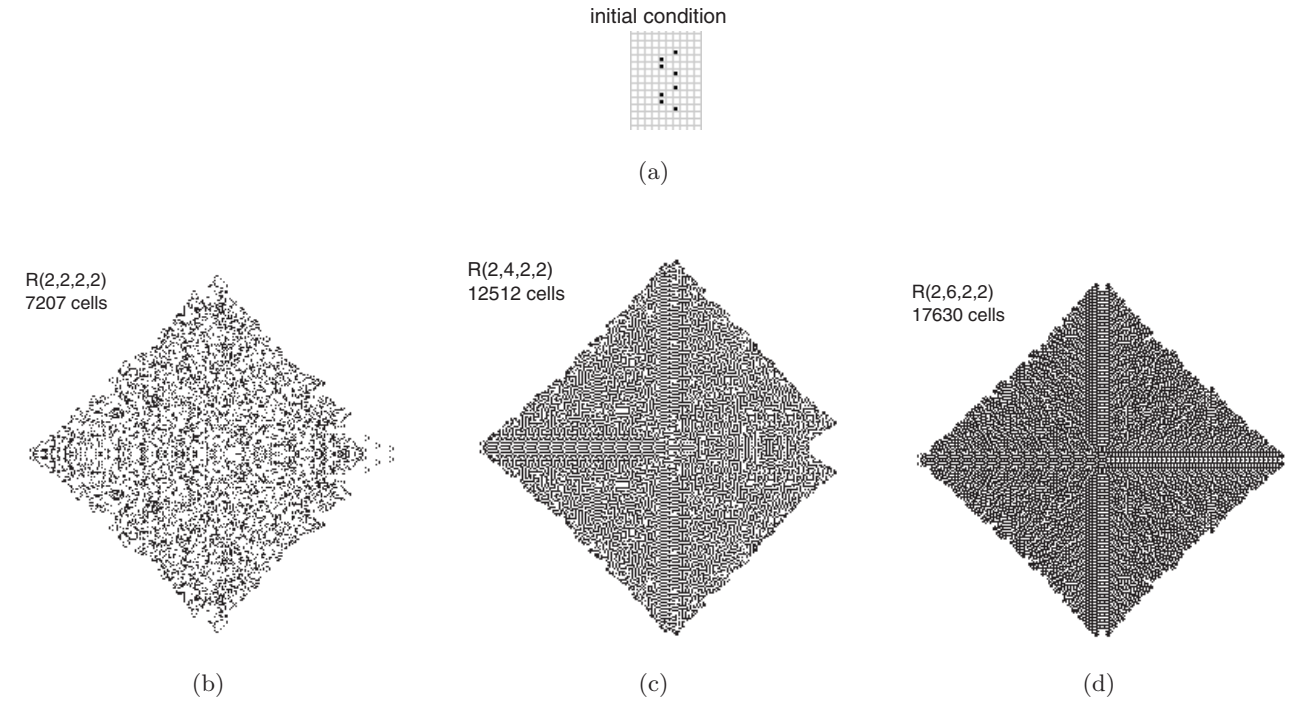

Fig. 23. Exemplar reaction–diffusion patterns produced by two associated gliders (like puffer train), configurations recorded at time step 120.

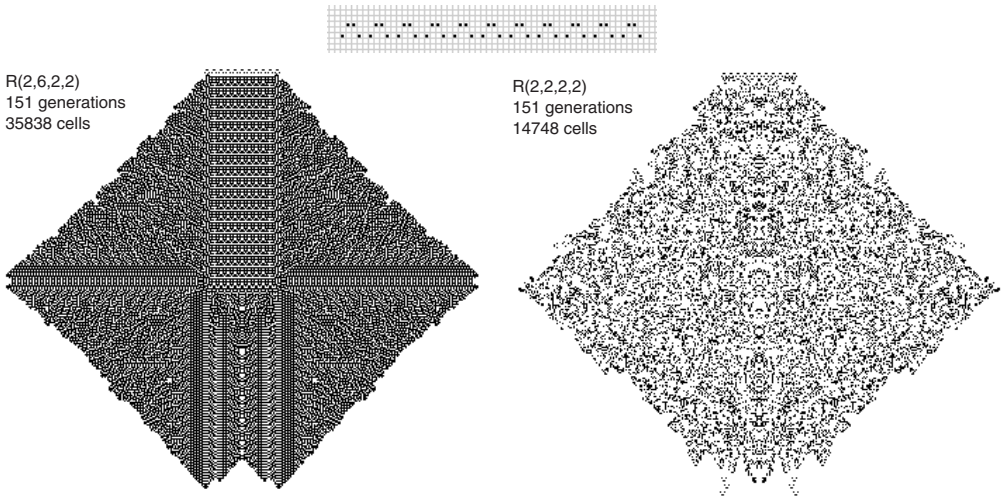

(a)

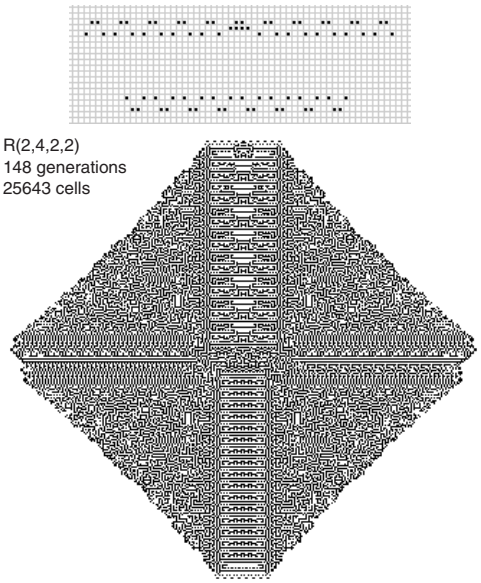

(b)

Fig. 24. Examples of patterns generated by glider compositions (puffer trains). Initial configuration of colliding gliders is shown at the top of each subfigure.

chaotic-looking. The quasi-symmetry is broken and no more gliders are generated as a result of the collisions when $c > 2$. The western part of the growing pattern becomes a combination of few domains of ordered 0-1-state tiles, while the eastern part either obeys labyrinthine structure ($R(2422)$) or labyrinthine domain with embedded ordered domains ($c > 4$). The growing reaction–diffusion patterns hold a memory of the collision.

In Fig. 23 we can see a range of reaction–diffusion patterns produced as an interaction of two gliders traveling side-by-side to the west like puffer train configuration. For rule $R(2222)$ a flotilla of six gliders traveling eastwards is generated. In configuration generated by CA with rule $R(2422)$ eastward part of the diffusing wave-front is concave, which is extremely unusual and had never been observed before. For all rules of Life 2c22 two initial gliders continue their travel west undisturbed, they are just

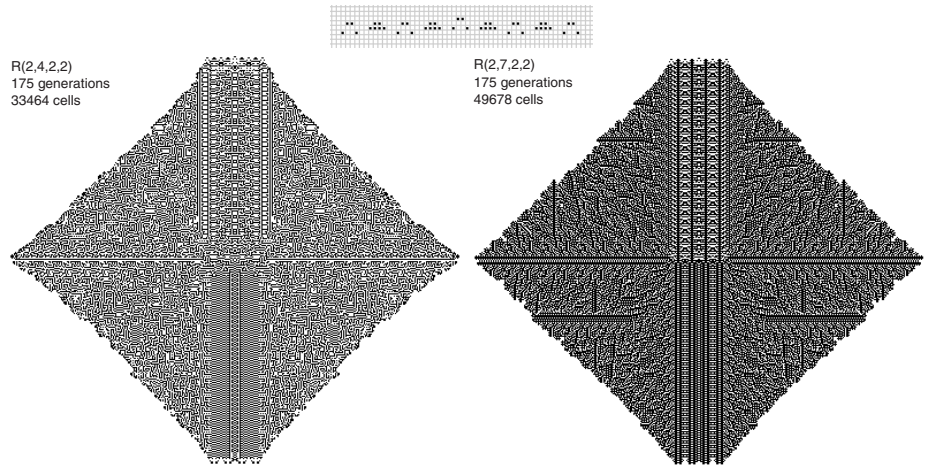

(a)

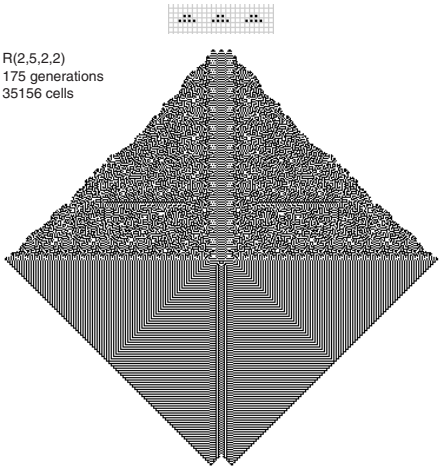

(b)

Fig. 25. Examples of patterns generated by glider compositions (puffer trains). Initial configuration of colliding gliders is shown at the top of each subfigure.

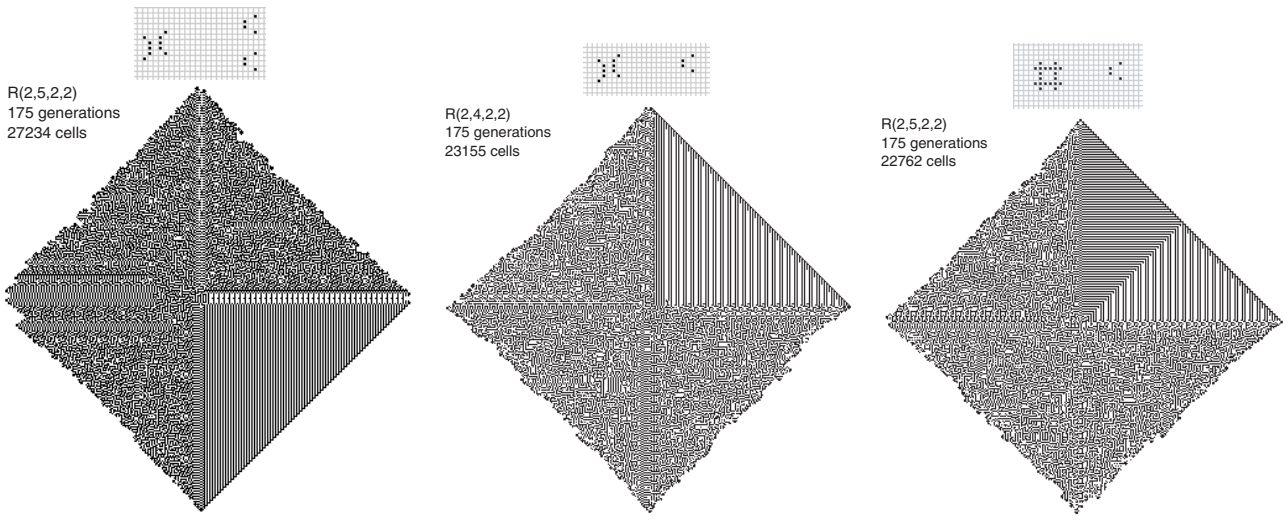

(a) (b) (c)

Fig. 26. Examples of patterns generated by (a) two gliders colliding with blinker, (b) one glider colliding with blinker, (c) one glider colliding with still life. Initial configuration of colliding gliders is shown at the top of each subfigure.

followed by growing fronts of the reaction–diffusion patterns.

Several examples of patterns generated by mobile structures composed of several gliders, and also between gliders, blinkers and still life are shown in Figs. 24–26. Outcomes of proximal interaction of several gliders are illustrated in Fig. 24(a), rules $R(2622)$ and $R(2222)$. Figure 24(b) demonstrates a pattern generated by an extension of glider row (puffer train) where one puffer train is inserted into the central part of another puffer train; the configuration exhibits certain types of macro-cells like domains produced due to interactions of sub-patterns produced by two puffer trains traveling in opposite directions. Collisions between gliders and stationary patterns (blinkers and still lifes) produce a combination of uniform, chaotic and ordered domains in the same reaction–diffusion pattern (bottom examples in Fig. 26).

6. Excitable Automata

We did not discuss yet another class of association-dissociation CA, namely the situation when $1 \leq \theta_1 \leq \theta_2 \leq 8$ but $\delta_1 = \delta_2 = 9$. In the framework of association-dissociation rule, neither lower nor upper boundaries of interval $[\delta_1, \delta_2]$ can take value nine because there are just eight neighbors in cell neighborhood, however in this case cell in state 1 will always (unconditionally, independent of states of its neighbors) take value 0. This is similar to an excitable CA but without a refractory state, 1 is an excited state, 0 is a resting state. For $\theta_1 \geq 3$ a random initial configuration (with low ratio of 1-state cells) will evolve to a configuration that is empty or contains just few breathing or blinking domains. For $\theta_1 \leq 3$ the dynamics of automata resemble "classical" excitation dynamics of 2D CA with interval (not threshold) excitation, studied in full detail in [Adamatzky, 2001]. Example configurations generated from random configuration are shown in Fig. 27. For $\theta_1 = 1$ and $\theta_2 = 1$, the automaton exhibits filaments of excitation (e.g. configuration 11 in Fig. 27), which are "transformed" to a more conventional target (e.g. configuration 18 in Fig. 27), or spiral (e.g. configuration 28 in Fig. 27) waves.

Cell state rule determined by interval $[\theta_1, \theta_2] = [22]$ allows for the existence of mobile self-localizations, or gliders. Minimal glider consists of four cells in state 1, and can move in four directions, below is an example of glider traveling west:

A minimal stationary localization is a blinker of two cells in state 1:

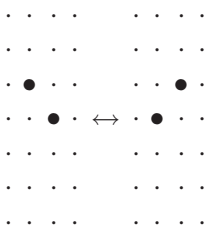

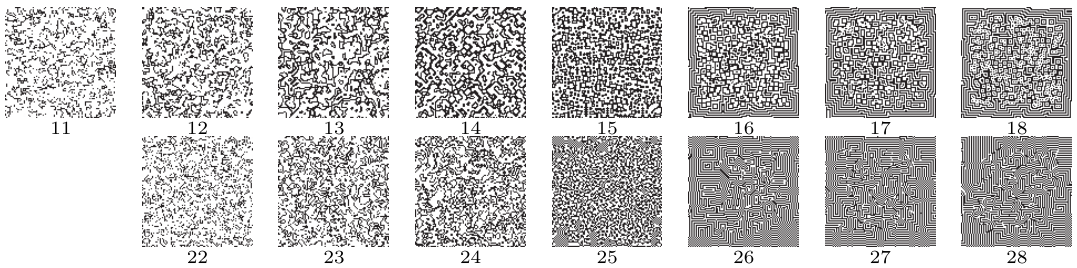

Fig. 27. Configurations of 2D 100×100 cells simply excitable CA, developed from initial random configuration (with 10% of cells in state 1) after 100 steps; each configuration is signed by two digits representing values of θ_1 and θ_2.

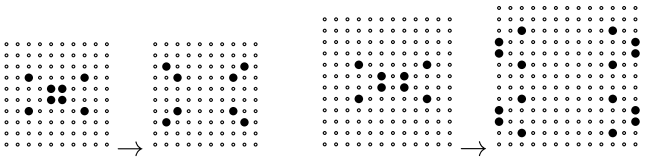

(a) (b)

Fig. 28. Outcomes of "head-on" collisions of gliders, initial position of gliders is shown on left configuration of each subfigure; resultant configurations — on the right of each subfigure. (a) Even distance between gliders, nil side-shift. (b) Odd distance between gliders, nil side-shift.

A minimal stimulus of "excitation" is two neighboring cells in state 1. Head-on collisions between gliders have various outcomes depending on odd-even distance, or "phase-difference", between colliding gliders and their side-shifts relative to each other. Basic examples are shown in Figs. 28 and 29.

Two gliders colliding head on at even distance annihilate and produce quadruple of blinkers [Fig. 28(a)], while those colliding at odd distance are multiplied [Fig. 28(b)].

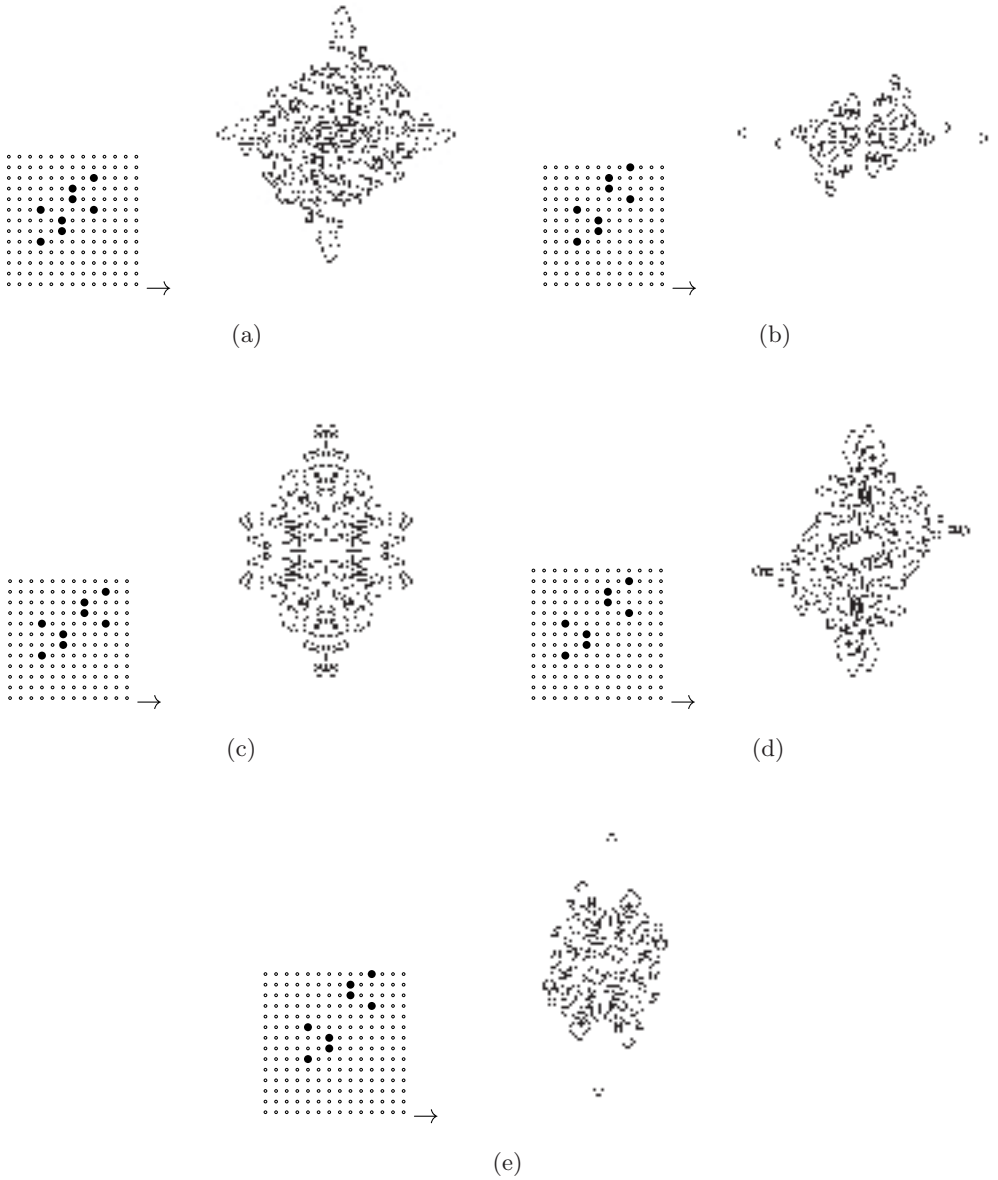

(a) (b) (c) (d) (e)

Fig. 29. Outcomes of "head-on" collisions of gliders, initial position of gliders is shown on the left configuration of each subfigure; resultant configurations — on the right of each subfigure — are recorded at step 50th, lattice size 120×120. (a) Odd distance, side-shift 3. (b) Odd distance, side-shift 4. (c) Even distance, side-shift 3. (d) Even distance, side-shift 4. (e) Even distance, side-shift 5.

Situations with head-on shift-shifts collisions, which do not result in just annihilation of gliders, are demonstrated in Fig. 29; for side-shifts more than 4 (for odd distance) or more than 5 (for even distance) gliders do not interact. When gliders are shifted relatively to each other, they produce spreading patterns, led, in most cases by gliders with extensive "tail-waves" attached. For situations (b) and (e) in Fig. 29, the speed of growing patterns is lower than speed of glider traveling, for other situations, both gliders and the growing patterns have the same speed.

7. Discussion

We studied two-dimensional cellular automata with binary cell states and eight cell neighborhoods, where every cell in state 0 takes state 1 if the number of neighbors in state 1 belong to interval $[\theta_1, \theta_2]$, and the cell in state 1 remains in state 1 if the number of neighbors in state 1 belongs to interval $[\delta_1, \delta_2]$, $1 \leq \theta_1 \leq \theta_2 \leq 8$, $1 \leq \delta_1 \leq \delta_2 \leq 8$.

The model can be interpreted as reaction–diffusion quasi-chemical system with substrate 0 and reagent 1, and $[\theta_1, \theta_2]$ is the interval of diffusion and $[\delta_1, \delta_2]$ is the interval of reaction. Exhaustive analysis of configurations generated for all 1296 rules allowed us to draft a morphological classification of the rules, and show that increasing the upper boundary of diffusion interval usually lead CA to make a transition from complex ordered spatio-temporal behavior to disordered behavior. An example is given in Fig. 30 where narrow intervals of reaction, (a) and (b), demonstrate order, while wider intervals of reaction, (c) and (d), disorder.

We have also studied precipitating and excitable automata, rules of which fell out of the definition of reaction–diffusion CA. We have shown that in the precipitating automaton increasing the interval of diffusion causes transition from disordered to labyrinthine to uniform domains. While increasing lower boundary of reaction interval causes transition from disordered and labyrinth/ordered to sparse patterns.

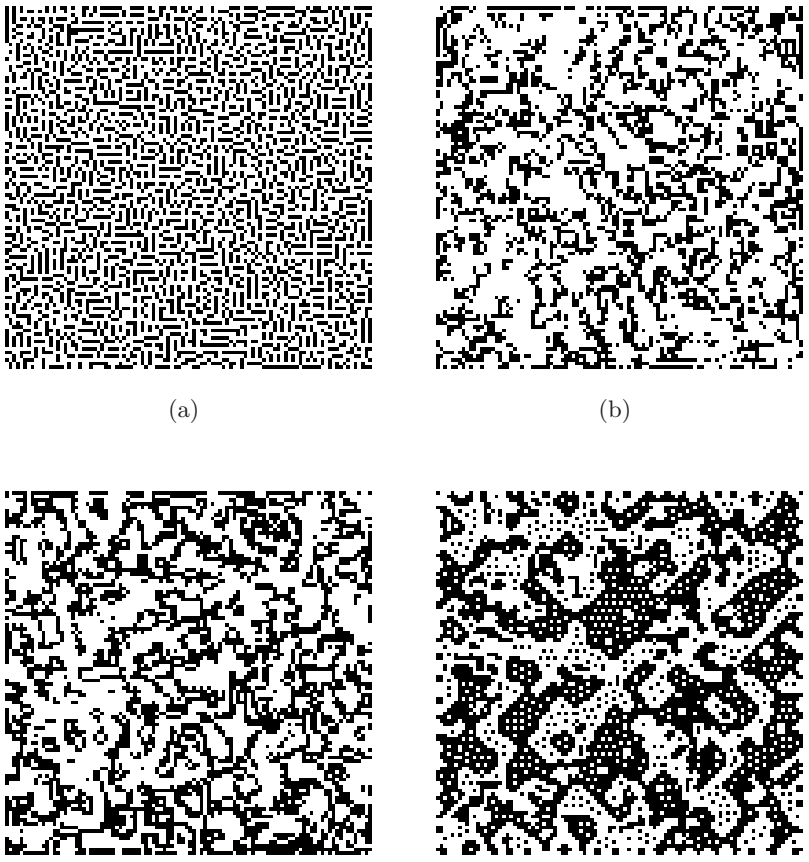

(a) (b) (c) (d)

Fig. 30. Configurations generated by rules (a) $R(1311)$, (b) $R(1212)$, (c) $R(1313)$, (d) $R(1318)$.

Amongst 1296 rules of cell-state transition of association–dissociation CA we have selected a set of rules — called Life 2*c*22 — diffusion interval is a singleton 2, and reaction interval has lower boundary 2 and a larger upper boundary — that support the existence of mobile traveling and stationary localizations — gliders, blinkers and still lifes. In most cases, interaction between localizations leads to the formation of growing reaction–diffusion patterns, the topology of which preserves a memory of the collisions which initiated them. A similar phenomenon was observed before in computational models [Adamatzky, 2004] and laboratory experiments [De Lacy Costello & Adamatzky, 2005] with subexcitable Belousov–Zhabotinsky chemical medium. There compact traveling localizations, wave-fragments, sometimes collided with each other and merged into a wave-fragment growing "indefinitely" till collision with boundaries of its chemical reactor. The growing wave-fragments in excitable chemical systems are memoryless, in general, it is impossible to reconstruct positions of compact wave-fragments which generated the growing pattern in their collision. Therefore, a more detailed study to Life 2*c*22 is in progress.

We can also mention dynamical complements (Fig. 31) of morphology-based classification. **E**-, **V**- and **C**-classes are characterized by stable orbit (uniform behavior) with nill density of cells in state 1. The periodic orbit is typical for classes **S**, **L**, **O** and **C**: configurations there are usually dominated by stationary localizations, still life and cycle life, patterns not existing in one-dimensional automata. **M**-class is a class of *u*nstructure and *u*nstable chaotic density. Quasi-stable density is typical for **P**-class where cellular space is dominated by quasi-periodic regions. Class **G** is characterized by "indefinite" density and complex behavior.

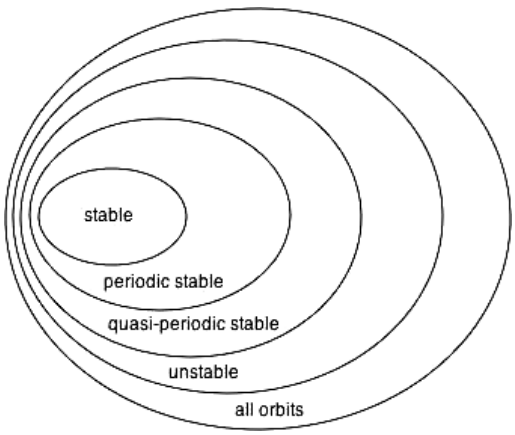

Fig. 31. Diagram of dynamical complements of morphological classification.

Also, regarding diffusion patterns formed by several gliders in a row, or puffer train, we are concerned — if a growth of reaction–diffusion patterns generated can be nonstationary? Do stationary or mobile generators of localizations, glider guns, exist in our models of reaction–diffusion CA? Also, it will be very important to find experimental analogies of chemical systems equivalent to reaction–diffusion automata, numerical simulations [Yang *et al.*, 2004] hint that morphological classes similar to that generated in our models can be produced in real-life chemical systems.

Yet another possible practical benefit of the discussed reaction–diffusion CA is in silicon implementation of reaction–diffusion processors. So far, a majority of the LSI circuits, see [Chua, 1999; Suzuki *et al.*, 2006] employ either discretized (cellular neural networks) or numerical integration of partial differential equations. However, as we demonstrated in the paper, even wider range of reaction–diffusion patterns can be generated in the studied CA. CA based architectures of LSI circuits will offer greater speed up, more precise tuning and manufacturing simplicity.

Acknowledgments

We thank Harold V. McIntosh for inspiration and advice and the British Council in Mexico for financial support for Dr. G. Martínez to visit UWE.

References

Adamatzky, A. [1995] "Computation of discrete convex hull in homogeneous automata networks," *Neural Network World* **3**, 17–25.

Adamatzky, A. [1998] "Universal dynamical computation in multi-dimensional excitable lattices," *Int. J. Theor. Phys.* **37**, 3069–3108.

Adamatzky, A. [2001] *Computing in Nonlinear Media and Automata Collectives* (Institute of Physics Publishing).

Adamatzky, A. (ed.) [2003] *Collision Based Computing* (Springer).

Adamatzky, A. [2004] "Collision-based computing in Belousov–Zhabotinsky medium," *Chaos Solit. Fract.* **21**, 1259–1264.

Adamatzky, A., De Lacy Costello, B. & Asai, T. [2005a] *Reaction-Diffusion Computers* (Elsevier).

Adamatzky, A., Wuensche, A. & De Lacy Costello, B. [2005b] "Glider-based computing in reaction–diffusion hexagonal cellular automata," *Chaos Solit. Fract.* **27**, 287–295.

Bell, D. I. [2000] *HighLife — An Interesting Variant of Life*, Article for review received by life@cs.arizona.edu, April 17, 1994.

Berlekamp, E., Conway, J. & Guy, R. [1982] *Winning Ways*, Vol. 2 (Academic Press).

Chua, L. [1999] *CNN: A Paradigm for Complexity* (World Scientific, Singapore).

De Lacy Costello, B. & Adamatzky, A. [2005] "Experimental implementation of collision-based gates in Belousov–Zhabotinsky medium," *Chaos Solit. Fract.* **25**, 535–544.

Gardner, M. [1970] "Mathematical games — The fantastic combinations of John H. Conway's new solitaire game of life," *Sci. Amer.* **223**, 120–123.

Hardouin Duparc, J. [1985] "Generalization of 'life'," in *Dynamical Systems and Cellular Automata* (Academic Press, London).

Jakubowski, M. H., Steiglitz, K. & Squier, R. [2001] "Computing with solitons: A review and prospectus," *Multiple-Valued Logic, Special Issue on Collision-Based Computing* **6**.

Langton, C. G. [1984] "Self-reproduction in cellular automata," *Physica D* **10**, 135–144.

Magnier, M., Lattaud, C. & Heudin, J.-C. [1997] "Complexity classes in the two-dimensional life cellular automata subspace," *Compl. Syst.* **11**, 419–436.

Martínez, G. J. [2000] Teoría del Campo Promedio en Autómatas Celulares Similares a "The Game of Life", Tesis de Maestría (CINVESTAV-IPN, México) http://delta.cs.cinvestav.mx/∼mcintosh/comun/tesis-maestria/genaro/thesis.html

Packard, N. H. & Wolfram, S. [1985] "Two-dimensional cellular automata," *J. Stat. Phys.* **38**, 901–946.

Rendell, P. [2003] "Turing universality of the game of life," *Collision Based Computing* (Springer), pp. 513–539.

Suzuki, Y., Takayama, T., Motoike, I. N. & Asai, T., [2006] "Striped and spotted pattern generation on reaction-diffusion cellular automata — theory and LSI implementation," *Int. J. Unconvent. Comput.* **2**, in press.

Toffoli, T. & Margolus, N. [1987] *Cellular Automata Machines* (MIT Press, Cambridge, MA).

Turing, A. M. [1952] "The chemical basis of morphogenesis," *Philos. S. Trans. Roy. Soc. London, Series B*, **237**, 37–72.

von Neumann, J. [1966] *Theory of Self-Reproducing Automata*, ed. Burks, A. W. (University of Illinois Press, Urbana and London).

Wolfram, S. [2002] *A New Kind of Science* (Wolfram Media, Inc., Champaign, Illinois).

Wuensche, A. [2004] Self-reproduction by glider collisions: The beehive rule, *ALife 9 Proc.* (MIT Press), pp. 286–291.

Yang, L., Zhabotinsky, A. M., & Epstein, I. R. [2004] "Stable squares and other oscillatory Turing patterns in a reaction–diffusion model," *Phys. Rev. Lett.* **92**, 19833-01.